Development, Growth & Differentiation
The Japanese Society of Developmental Biologists

Develop. Growth Differ. (2013) **55**, 247–259 doi: 10.1111/dgd.12029

Original Article

Physarum polycephalum mutants in the photocontrol of sporulation display altered patterns in the correlated expression of developmentally regulated genes

Viktoria Rätzel, Britta Ebeling, Xenia-Katharina Hoffmann,† Jens Tesmer† and Wolfgang Marwan*

Magdeburg Centre for Systems Biology and Lehrstuhl für Regulationsbiologie, Otto-von-Guericke-Universität, Magdeburg, 39106, Germany

Physarum polycephalum is a lower eukaryote belonging to the amoebozoa group of organisms that forms macroscopic, multinucleate plasmodial cells during its developmental cycle. Plasmodia can exit proliferative growth and differentiate by forming fruiting bodies containing mononucleate, haploid spores. This process, called sporulation, is controlled by starvation and visible light. To genetically dissect the regulatory control of the commitment to sporulation, we have isolated plasmodial mutants that are altered in the photocontrol of sporulation in a phenotypic screen of *N*-ethyl-*N*-nitrosourea (ENU) mutagenized cells. Several non-sporulating mutants were analyzed by measuring the light-induced change in the expression pattern of a set of 35 genes using GeXP multiplex reverse transcription–polymerase chain reaction with RNA isolated from individual plasmodial cells. Mutants showed altered patterns of differentially regulated genes in response to light stimulation. Some genes clearly displayed pairwise correlation in terms of their expression level as measured in individual plasmodial cells. The pattern of pairwise correlation differed in various mutants, suggesting that different upstream regulators were disabled in the different mutants. We propose that patterns of pairwise correlation in gene expression might be useful to infer the underlying gene regulatory network.

Key words: cell differentiation, gene expression, gene regulatory network, multiplex reverse transcription-polymerase chain reaction, *Physarum polycephalum*.

Introduction

Physarum polycephalum is an acellular slime mold that phylogenetically belongs to the amoebozoa group of organisms (Baldauf & Doolittle 1997; Baldauf *et al.* 2000; Barrantes *et al.* 2010). *Physarum* can differentiate into various structurally, functionally, and biochemically different cell types that occur in temporal order in the course of the branched life cycle (Burland *et al.* 1993). At one stage of the life cycle, haploid, mononucleate amoebae, also called myxamoebae, hatch from mature spores. Myxamoebae feed on bacteria and propagate by mitosis. Two amoebae of different mating types may mate with each other to form a diploid zygote. The zygote develops into a diploid multinucleate plasmodium, which grows as long as sufficient nutrients are available. During growth, the protoplasmic mass continually increases and the nuclei suspended in the vigorously streaming protoplasm synchronously divide by undergoing a closed mitosis, while the plasmodial cell does not divide. A plasmodium covering a 9 cm diameter Petri dish, for example, then contains between 10^7 and 10^8 nuclei, which are still naturally synchronous in cell cycle progression and during differentiation (Rusch *et al.* 1966; Sachsenmaier *et al.* 1972; Werenskiold *et al.* 1988).

In response to starvation, the plasmodium has two options of development to exit from growth and proliferation by forming dormant, drought-resistant cell types. The developmental decisions are under sensory control and involve the differential regulation of developmental genes (Putzer *et al.* 1983, 1984; Martel *et al.* 1988). The plasmodium may either form macro-cysts also called sclerotia or it may sporulate. During sporu-

*Author to whom all correspondence should be addressed.
Email: wolfgang.marwan@ovgu.de
†These authors contributed equally to this work.
Received 14 August 2012; revised 6 November 2012; accepted 6 November 2012.

lation the entire protoplasmic mass synchronously develops into fruiting bodies. In the fruiting bodies the protoplasm is cleaved, the nuclei undergo meiosis and give rise to mononucleate, haploid spores.

Experimentally, sporulation can be triggered with a pulse of far-red light, which is sensed by a phytochrome-like photoreceptor (Starostzik & Marwan 1995a; Lamparter & Marwan 2001). Approximately 4–6 h after the inductive light pulse, the plasmodium has crossed the point of no return to become irreversibly committed to sporulation. Before commitment, the plasmodium can return to the proliferative state when it is supplemented with glucose (Starostzik & Marwan 1994, 1995b). The transcriptomic changes that occur in committed cells have been analyzed by massive parallel sequencing (Barrantes *et al.* 2010).

The Mendelian genetics of *Physarum* is well established (for review see [Dee 1987]). By treatment of mononucleate, haploid amoebal cells with UV or chemical mutagens, mutants can be obtained, crossed with wild type amoebae and, after meiotic recombination in a sporulating plasmodium, segregants can be screened for phenotypes and genotypes (Schedl & Dove 1982; Dee 1987). Massive parallel sequencing combined with polymerase chain reaction (PCR)-based techniques would allow modern genetic analyses to be performed at the molecular level.

The isolation and characterization of mutants is greatly facilitated by a temperature-sensitive allele, which is closely linked to the mating type locus *matA,* and which causes apogamic development (Dee 1966, 1987; Wheals 1970; Mohberg 1977). By apogamic development, a haploid amoebal cell can directly transform into a haploid plasmodium without the need of mating. This provides the practical advantage that plasmodia arising from amoebal mutant clones can be directly screened for phenotypes, while crossing of the mutants with other strains and subsequent Mendelian analysis is still possible at the temperature that blocks apogamic development.

Here, we isolate mutants in the photocontrol of sporulation and show that these mutants display altered gene expression patterns in response to light and altered patterns in the pairwise correlation of differentially expressed genes.

Materials and methods

Screen for mutants altered in the photocontrol of sporulation

Amoebae of the apogamic wild-type strain WT31 were mutagenized with *N*-ethyl-*N*-nitrosourea (ENU) as described (Sujatha *et al.* 2005). After mutagenesis, cells were allowed to undergo several cell divisions and after forming a confluent amoebal layer, develop into cysts. The cysts were used to prepare glycerol stocks of the mutant library. All manipulations were performed under sterile conditions (Sujatha *et al.* 2005).

Aliquots from a glycerol stock of a mutant library were thawed and diluted 100- to 1000-fold in order to obtain approximately 20–50 amoebal colonies per plate. The cyst suspension was examined under the microscope without a cover slip to verify that cysts were suspended individually and did not form any clumps. Before use, microscope slides were thoroughly cleaned with ethanol to remove any detergent from the surface that might dissociate potential clumps of cysts during sample preparation. Avoiding clump formation is essential in order to make sure that each amoebal colony emerges as a clone of a single cell. 100 μL of the diluted amoebal cyst suspension were mixed on a plate with 100 μL of a standardized formalin-killed *E. coli* suspension that served as a food source for the amoebae (FKB; [Dee 1986]) and the droplet was spread evenly over a DSPB agar plate (diluted semidefined phosphate buffered medium; [Anderson *et al.* 1997]) by streaking with the conical tip of a 10-mL glass pipette. The plates were incubated at 24°C for 48 h to facilitate hatching of amoebae from cysts and subsequently at 30°C to allow amoebal growth while suppressing the unwanted formation of haploid plasmodia by apogamic development (Bailey *et al.* 1987, 1992; Bailey 1995). After several days at 30°C, amoebal colonies became visible. Well separated individual colonies were picked by suspending them in a droplet of 10 μL of FKB by pipetting up and down several times. The droplet with the picked cells was split into two parts each mixed with a droplet of 100 μL FKB that had been placed on a DSPB as well as on a small (diameter = 4.5 cm) DSDM (diluted semidefined medium; [Dee *et al.* 1997]) agar plate. The suspensions were spread over the plates to obtain even amoebal growth.

The DSPB plate was incubated for 2 days at 24°C and subsequently for 10 days at 30°C to allow amoebal growth and encystment. Each plate with encysted amoebae was flooded with 10 mL of a 15% (v/v) aqueous glycerol solution. The cysts were suspended with the help of a 10-mL glass pipet and a 1-mL aliquot was frozen at –80°C to preserve the amoebal clone.

The DSDM plate was incubated at 24°C for several days to allow amoebal growth and the apogamic development of small plasmodia, which were inoculated on a SDM plate (semidefined medium; [Dee *et al.* 1997]), to obtain a fully grown macro-plasmodium from which further cultures were inoculated.

Each plasmodial clone was then inoculated onto one SDM plate covered with a sheet of filter paper (diame-

ter = 70 mm, 85 g/m^2; Macherey Nagel 640 m, supplied by Carl Roth, Germany). Each plate was incubated for several days at 24°C until it was completely covered by a fully grown plasmodium. The filter paper with the plasmodium was transferred to a sporulation agar plate for starvation at 22°C in complete darkness. The incubation temperature is critical to avoid light-independent sporulation in the wild type. After 6 days of starvation in the dark, plasmodia were examined for spontaneous (i.e. light-independent) sporulation under dim green safe light to identify potential mutants that sporulate spontaneously. Plasmodia that had not sporulated after starvation (the vast majority) were irradiated for 30 min with far-red light ($\geq$700 nm; 13 W/m^2) as described (Starostzik & Marwan 1998). Those plasmodia that had not sporulated on the next day were immediately exposed to a second 30-min pulse of far-red light, and eventually to a third one if the second pulse did not cause sporulation within one day. The screening procedure (with potentially three subsequent light exposures, one exposure each day) was repeated twice for all clones. This screening was found to be selective enough to identify potential mutants in the photocontrol of sporulation that cause a tight phenotype.

To verify the phenotypes and the stability of potential mutants, plasmodia were regrown from glycerol stocks of amoebal clones. From each candidate strain, 10 amoebal subclones were picked and allowed to apogamically develop into plasmodia. Five plasmodia of each subclone were used to verify the phenotype as described for the screening procedure. After successful verification, a plasmodial strain developed from one subclone of each identified mutant strain was taken into liquid shaken culture for the generation of spherules and for further phenotypic characterization. Cultures on plates were incubated in Memmert ICP 800 incubators (Memmert, Schwabach, Germany). As the incubation temperatures are critical, they were verified using a calibrated mercury thermometer with 0.1°C resolution. The incubators were supplied with 0.5 volumes of air per hour, which was dehumidified by passing the airflow through a reflux condenser with steel-made cooling coil thermostated at 2°C. Supply with dry air contributes to the reproducible culture conditions and helps to avoid that plasmodia creep out of the culture dishes at high humidity.

Growth and preparation of sporulation-competent plasmodia for gene expression studies

A 5-L fermenter (Minifors, Infors HT, Bottmingen, Switzerland) with 1.5 L of growth medium (Daniel & Baldwin 1964) was inoculated with 2 vol % of a 3.5-day-old shaken culture. Plasmodia were grown for 4 days at 24°C, supplied with 1 L of air per min, and stirred at 250 rpm with a marine propeller. Microplasmodia were harvested, washed twice with salt medium, and applied to starvation agar plates (9 cm diameter) with niacin and niacinamide (Daniel & Rusch 1962) as described (Starostzik 1995; Starostzik & Marwan 1998). A ring of 1 g of cell paste (fresh weight) was applied to the centre of each plate with the help of a motor-driven 50-mL syringe coupled to an automatic device for rotating the agar plate around its axis. Plates were incubated for 6 days at 22°C in complete darkness. The incubation temperature is critical in order to avoid unwanted spontaneous sporulation in response to heat.

Induction of sporulation, preparation of total RNA, and multiplex gene expression profiling

Sporulation of competent plasmodia was induced by a far-red light pulse (30 min, $\lambda \geq 700$ nm, 13 W/m^2) as described (Starostzik & Marwan 1998). At 6 h after the onset of the light pulse, three quarters of each plasmodium were harvested with a small glass spoon (Roth, Karlsruhe, FRG), shock-frozen in liquid nitrogen and stored at –80°C for RNA isolation. One quarter was maintained in the dark for another 18 h to reveal the developmental decision (i.e. whether or not sporulation occurred). Control plasmodia were treated identically except that the light pulse was omitted (dark control). All manipulations were done under sterile conditions and under green safe light as described (Kroneder *et al.* 1999). For extraction of total RNA, approximately 100 mg fresh weight material of a single plasmodium was used. Samples were homogenized quickly at room temperature for 10 s in 3-mL peqGOLD TriFast (PeqLab; Nr 30-2020) using a glass potter and incubated for further homogenization for 1 min at 50°C. RNA was extracted with phenol/$CHCl_3$ using 15 mL Phase Trap tubes according to manufacturer's instructions (PeqLab; Nr 30-0150A-01). Afterwards the RNA was precipitated with ethanol, and digested with rDNase to remove DNA contamination as described (Hoffmann *et al.* 2012).

Multiplex RT–PCR reactions were performed to simultaneously amplify 35 transcripts and the amplification products were quantified through separation of the fragments on a Beckman Coulter 8-capillary sequencer (CEQ 8800) as described (Hoffmann *et al.* 2012). Each series of samples to be directly compared to each other was analyzed with the same gene expression profiling (GeXP) kit to ensure consistent results. For each GeXP kit used, a new calibration curve was established as described in order to correct for variations in the quality of the kit components.

Computational methods, statistics, and software used

GEDI analysis. GEDI maps were computed with the Gene Expression Dynamics Inspector v2.1, a platform-independent software package (http://www.childrenshospital.org/research/ingber/GEDI/gedihome.htm) as described in the following. The expression values of the set of 35 genes as measured in all samples of a given strain (wild type or mutant) were normalized to the average expression level of the reference genes *dspA*, *ribB*, and *damA*. Then, the gene expression data measured for all plasmodial samples (wild type and mutants) were combined into one comprehensive dataset on which the algorithm was executed. Accordingly, the relative changes in the colour patterns of the GEDI maps are fully comparable between all plasmodia of the entire dataset. A grid size of 4×4 was chosen so that the algorithm assigned at least one of the 35 genes to each of the 16 tiles. The resulting miniclusters defined genes that are coregulated in the wild type and the mutants.

Mann–Whitney U-*Test.* To define genes that were up- or downregulated in response to far-red light, the data were analyzed using the parameter-free Mann–Whitney *U*-Test (Mann & Whitney 1947). The U-value U_a characterizing the difference between the plasmodia of group a (e.g. dark control) with group b (e.g. far-red irradiated) was calculated according to

$$U_a = n_a \cdot n_b + \frac{n_a(n_a+1)}{2} - R_a$$

where n_a and n_b are the sample sizes of group a and group b, respectively, and R_a is the sum of ranks in group a. A threshold for the U-value of $U_a \geqq 0.05$ or $\leqq 0.05$ was chosen to indicate whether the light and the dark treated plasmodia form significantly different groups with respect to the relative concentration of any given transcript.

Pearson Correlation Test. The Pearson correlation (Rovine 1997) was used to reveal any pairwise correlation in the expression levels of the 35 genes. For 11 genes selected from the GEDI map, the correlation coefficient r was calculated according to

$$r = \sum_{i=1}^{n} \left(\frac{(x_i - \overline{x}) \cdot (y_i - \overline{y})}{(n-1) \cdot s_x \cdot s_y} \right)$$

where x and y are the expression levels of two different genes i and s_x and s_y are the standard deviations of the transcript abundance of gene x and gene y, respectively. Thresholds of $r \leq -0.8$ or $r \geq 0.8$ were chosen for negative or positive correlation to be significant.

Results

Isolation of mutants in the photocontrol of sporulation

Libraries of haploid amoebae mutagenized with ENU were screened for mutants in the photocontrol of sporulation (Fig. 1). Amoebal clones obtained as single colonies on agar plates were picked twice. One sample was used to propagate the amoebal clone for preservation as glycerol stock. In parallel, amoebae were allowed to develop apogamically into a plasmodium, which was grown to a macroplasmodium and then starved for 6 days in complete darkness. During the period of starvation, wild type plasmodia become competent for the induction of sporulation by far-red light, blue light, or heat shock (Starostzik & Marwan 1995b). After 6 days, plasmodia were screened for spontaneous, that is, light-independent sporulation. Plasmodia were inspected visually for altered plasmodial morphology and subsequently exposed to a far-red light pulse, which is saturating in inducing sporulation in the wild type. Plasmodia that spontaneously sporulated in the dark and those that did not sporulate in response to the far-red pulse were subjected to rounds of verification in order to identify mutants in the photocontrol of sporulation that display tight phenotypes. We screened libraries containing amoebae that were mutagenized once or twice, respectively. From 820 clones of the once mutagenized library two spontaneously sporulating mutants were obtained. Out of 500 clones from the twice mutagenized library, seven nonsporulating mutants were obtained (Table 1). Amoebal subclones retrieved from the glycerol stocks confirmed plasmodial phenotype and stability of the identified mutant strains. Mutants obtained in the present screen and those isolated in previous screens (Starostzik & Marwan 1998; Sujatha *et al.* 2005) were found to be phenotypically stable.

Gene expression analysis uncovers different molecular phenotypes of nonsporulating mutants

Transcriptomic studies (Barrantes *et al.* 2010) as well as quantitative multiplex RT–PCR (GeXP) analyses with RNA samples prepared from individual plasmodial cells (Hoffmann *et al.* 2012) have shown that at 6 h after induction by a far-red light pulse, that is, shortly downstream of the point of no return, the expression level of many genes has already changed drastically. Some genes are differentially regulated even at 2 h (Hoffmann *et al.* 2012) which is far upstream the point of

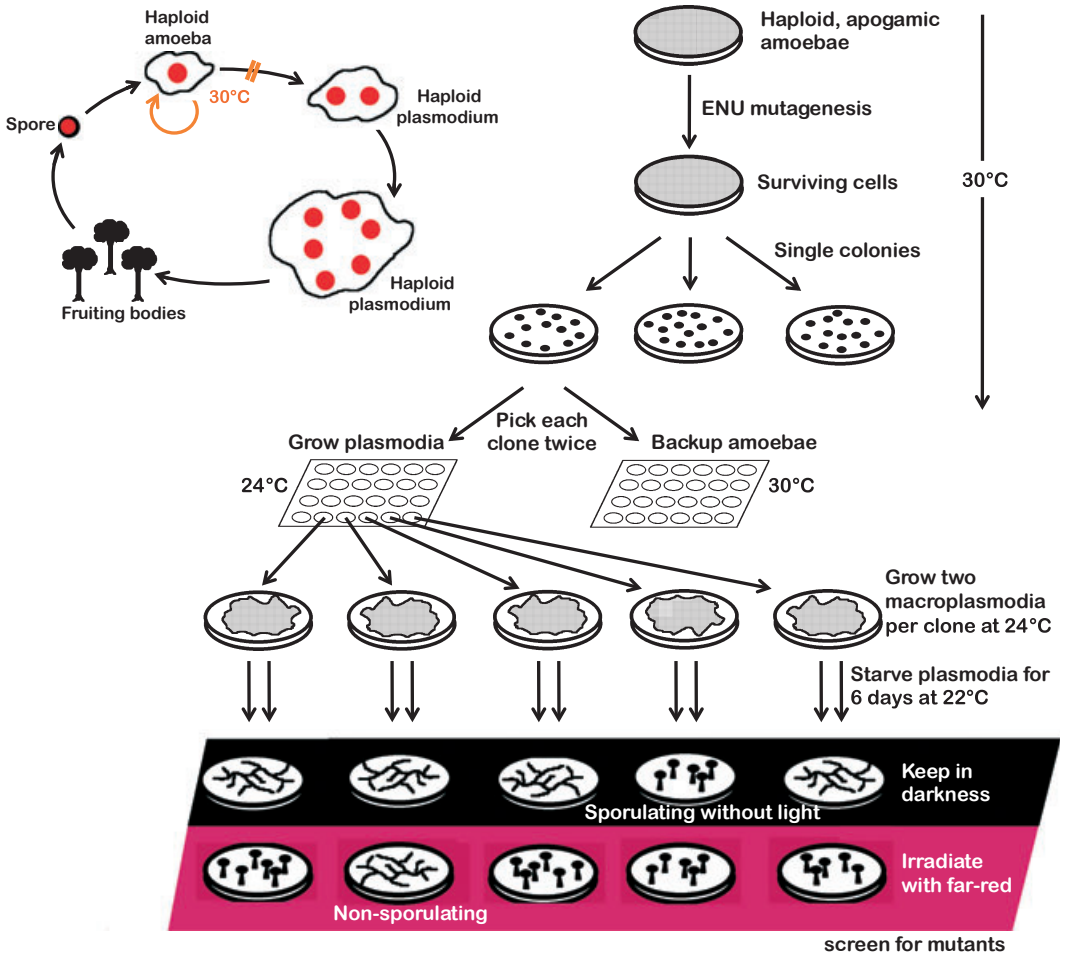

Fig. 1. Workflow of the genetic screen for mutants altered in the photocontrol of sporulation. Haploid, apogamic amoebae are transformed into flagellates, mutagenized, regrown, and plated. Single colonies are picked in duplicate for strain preservation as amoebal glycerol stocks and for growth of plasmodia through apogamic development. Plasmodia are starved for 6 days to gain sporulation competence and then screened for mutants that spontaneously sporulate in the absence of light and those that do not sporulate in response to far-red light. Amoebae are grown at 30°C in order to suppress apogamic development. The inset upper left shows the life cycle with apogamic development. At 30°C haploid amoebae can proliferate while the formation of haploid multinucleate plasmodia by apogamic development is blocked. Haploid plasmodia of the wild type show no detectable difference in the sensitivity for the induction of sporulation by far-red light as compared to diploid plasmodia that developed through mating of two amoebae of different mating type.

no return where sporulation of the induced plasmodium can still be prevented by feeding glucose (Starostzik & Marwan 1994, 1995b). This suggests that sensory signal transduction, signal processing at the protein level, and gene regulation at least to some extent are chronologically interwoven. Moreover, not all plasmodial cells that show a light-induced transcriptional response necessarily sporulate (Hoffmann *et al.* 2012). Therefore, it seemed likely that at least some of the nonsporulating mutants might have altered gene expression patterns and/or respond at the transcriptome level to the light stimulus even if sporulation subsequently cannot occur.

Wild type and mutant plasmodia starved for 6 days were irradiated with a 30 min pulse of far-red light. At 6 h after the light pulse, one quarter of each plasmodium was cut off together with its supporting agar slice, returned to the dark and checked on the next day, in order to see whether or not sporulation had occurred (Fig. 2). The other part was immediately shock-frozen in liquid nitrogen for subsequent isolation of RNA. In the dark controls irradiation was omitted but the samples were treated identically otherwise.

A set of 35 genes has been selected based on their differential regulation (up or down) during commitment of the wild type to sporulation and/or for encoding different types of proteins like kinases, lipases, checkpoint proteins, RNA-binding proteins etc. to cover different cellular processes (Table 2) (Hoffmann *et al.* 2012). Transcripts of the set were amplified by multi-

Table 1. Mutant strains and relevant phenotypes of the strains used

Strain	Relevant phenotype	Reference
WT31	Wild type	Starostzik & Marwan 1998;
PHO1	Strongly reduced sporulation in response to far-red	Starostzik & Marwan 1998;
PHO3	Strongly reduced sporulation in response to far-red	Sujatha *et al.* 2005
PHO48	Reduced sporulation in response to far-red	This work
PHO57	Strongly reduced sporulation in response to far-red	This work
PHO64	Strongly reduced sporulation in response to far-red	This work
PHO68	Strongly reduced sporulation in response to far-red	This work
PHO72	Reduced sporulation in response to far-red	This work
PHO76	Strongly reduced sporulation in response to far-red	This work

plex RT–PCR in the same cap and quantified through separation of the amplified fragments on a capillary sequencer (GeXP analysis) (Liu & Saint 2002; Rai *et al.* 2008; Hoffmann *et al.* 2012). The expression levels of each of the 35 genes relative to each other were evaluated for each sample (i.e. for each individual plasmodial cell).

Wild type and sporulation-deficient mutants were phenotypically characterized by analyzing, visualizing, and comparing the expression patterns of 35 genes. Data were analyzed and visualized with the Gene Expression Dynamics Inspector (GEDI) (Eichler *et al.* 2003; Guo *et al.* 2006), a software to cluster high dimensional gene expression data into a two-dimensional colour map. The method uses so-called self organizing maps (SOM) to generate patterns that are easily accessible to the human eye. The underlying algorithm clusters genes with similar expression patterns according to their Euclidian distance and arranges the resulting miniclusters with similar behavior adjacent to each other. Dynamic changes in gene expression patterns become therefore easily visible.

To generate the GEDI maps shown in Figure 3, we combined the expression values of all 35 genes measured in all plasmodial cells, wild type and mutants, into one dataset and executed the algorithm. As a result, the assignment of genes to the miniclusters and the geometric arrangement of the miniclusters relative to each other is the same in all maps shown. Each map corresponds to the expression pattern found in a different individual plasmodial cell. Therefore, not only the colour coded expression levels of the 35 genes, but also their expression patterns can be directly compared between individual plasmodial cells for the given experimental condition (dark control vs. far-red irradiated) but also between wild type and mutant strains. For the wild type the gene expression pattern differs drastically between the dark controls and the samples taken 6 h after far-red irradiation. Although some of the plasmodia within the far-red irradiated group as well as within the dark control group have quite similar expression patterns, there is also considerable individual variation between different plasmodial cells.

In the non-sporulating mutants the response to light was clearly different as compared to the wild type. In PHO1, PHO3, PHO57, and PHO76 there was only a slight still in some of the plasmodia a more pronounced response to the light stimulus. In PHO64 and PHO68 plasmodia the response to far-red at 6 h was very clear but still different as in the wild type.

In strains PHO48 and PHO72 some of the plasmodia sporulated in response to the light stimulus. Nevertheless, we classified this phenotype as tight as well, because the lack of sporulation in some of the plasmodia regularly occurred in response to a stimulus that is highly saturating in the wild type. Note that also in these mutants sporulation was always an all-or-none response for each individual plasmodial cell. The gene expression response of PHO48 and PHO72 to light,

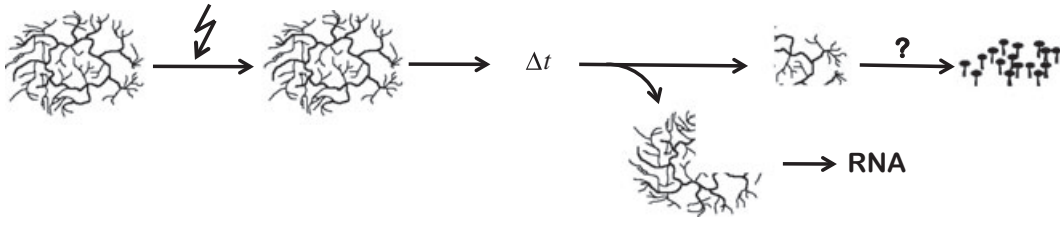

Fig. 2. Experimental protocol of sample preparation. Plasmodia starved for 6 days develop a veined network and gain sporulation competence. After application of a far-red light stimulus pulse of 30 min (flash symbol), the plasmodia are returned to the dark. At time Δt after the stimulus pulse, each plasmodium together with its supporting agar slice is cut into two pieces. Three quarters are frozen in liquid nitrogen for the subsequent isolation of RNA, and one quarter is maintained in the dark and checked for sporulation on the following day. In corresponding dark controls, the light stimulus was omitted.

Table 2. Genes analyzed for transcript abundance and their degree of similarity to orthologues in the Swissprot data base.

Gene	Similarity	Swissprot entry	E-value	Percentage query coverage
anxA	Annexin-B12	P26256	6.00E-041	98.00
ardA	Actin, plasmodial isoform	P02576	9.00E-109	69.00
arpA	Probable basic-leucine zipper transcription factor G	Q54RZ9	2.00E-012	29.00
cdcA	Cell division control protein 31	P06704	6.00E-027	38.00
cudA	Putative transcriptional regulator cudA	O00841	1.00E-023	38.00
damA	DNA damage-binding protein 1a	Q9M0V3	8.00E-100	87.00
dspA	Dual specificity protein phosphatase 12	Q9JIM4	1.00E-012	41.00
ehdA	EH domain-containing protein 1	Q641Z6	6.00E-025	94.00
gapA	Probable GTPase-activating protein 8	Q8H100	3.00E-023	52.00
hcpA	Histone chaperone ASF1A	Q2KIG1	5.00E-062	82.00
hstA	Probable histone H2B 4	Q27876	1.00E-041	43.00
ligA	Checkpoint protein hus1 homolog 1 (LigA)	Q54NC0	1.00E-028	94.00
meiB	Meiosis protein mei2	Q64M78.1	9.00E-064	27.00
nhpA	Non-histone chromosomal protein 6	Q4PBZ9	5.00E-017	30.00
pakA	Serine/threonine-protein kinase pakC	Q55GV3	3.00E-048	79.00
pcnA	Proliferating cell nuclear antigen	Q43124	9.00E-076	81.00
pikB	Phosphatidylinositol 3-kinase 2	P54674	3.00E-063	68.00
pikC	Phosphatidylinositol 4-kinase beta	Q49GP3	8.00E-050	94.00
pksA	Serine/threonine-protein kinase phg2	Q54QQ1	9.00E-035	89.00
pldA	Phosphatidylinositol-glycan-specific phospholipase D	Q8R2H5	4.00E-062	91.00
pldB	Phosphatidylinositol-glycan-specific phospholipase D	P80108	1.00E-080	83.00
pldC	Phospholipase D	Q9LRZ5	4.00E-014	61.00
pptA	Phosphatase DCR2	Q05924	6.00E-019	59.00
pptB	Protein phosphatase 2C POL	Q8RWN7	0.016	14.00
psgA	*Physarum* specific gene			
pumA	Pumilio homologue 2	Q80U58	2.00E-046	80.00
pwiA	Piwi-like protein 1	Q96J94	2.00E-055	92.00
ralA	Circularly permutated Ras protein 1	Q75J93.1	4.00E-017	58.00
rasA	Ras-related protein RABD2a	P28188	3.00E-029	49.00
rgsA	Regulator of G-protein signaling 2	O08849	3.00E-005	31.00
ribA	60S ribosomal protein L38	Q1HRT4	2.00E-017	40.00
ribB	60S ribosomal protein L4-2	Q54Z69	4.00E-036	66.00
spiA	Protein spire	Q9U1K1	1.00E-004	31.00
tspA	Tumor suppressor p53-binding protein 1	P70399	2.00E-004	16.00
uchA	Programmed cell death protein 2	Q2YDC9	1.00E-006	32.00

which was clearly different to the wild type, supports the use of the gene expression pattern as a mutant phenotype. In these strains (PHO48 and PHO72) a clear gene expression response to the light stimulus was not obvious for all plasmodia and the mutants behaved different as compared to the wild type in this respect as well.

Over the years it very rarely occurred that in strains PHO1 and PHO3 some of the plasmodia sporulated in response to light, suggesting that the mutation in these strains also influences the probability for sporulation to occur rather than abolishes the ability for sporulation *per se*.

Mutants show different patterns in the correlated expression of genes

The GEDI maps clearly show that there is a relatively high variation in the expression patterns between individual plasmodia of a given experimental group. High variation was even obvious in those cases where only few plasmodia have been analyzed. In some clusters of genes identified with GEDI analysis, up- or downregulated genes cluster together. It appeared that the expression levels of some of these genes are more or less strictly correlated in individual cells in the dark or in far-red irradiated samples although the relative abundance of the transcripts as compared to other messages can vary drastically and also change between dark controls and far-red irradiated plasmodial cells (Fig. 4). To obtain more comprehensive results, we arbitrarily picked from the strongly differentially regulated genes a subset of 11 genes from the GEDI miniclusters to perform a Pearson correlation analysis and to quantify the correlated expression of each gene with each other. In Figure 5 the correlations in gene expression are graphically represented setting a threshold for the correlation coefficient of $r = 0.8$. In the wild type there is a clear correlation in gene expression levels in and in between the groups of upregulated and downregulated genes. The expression levels of *cdcA* and

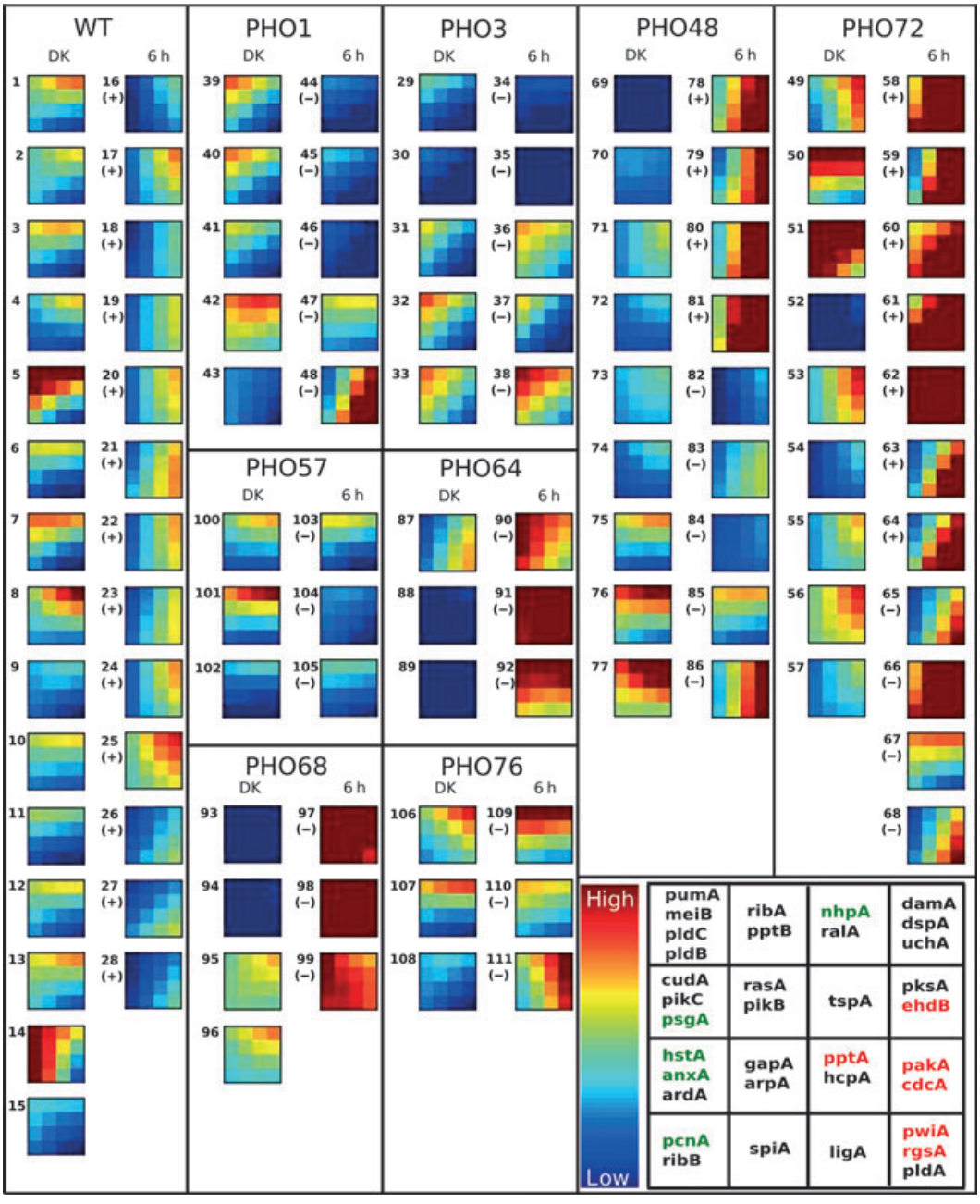

Fig. 3. Gene Expression Dynamics Inspector (GEDI) maps of the gene expression patterns of individual plasmodial cells of wild type and mutants. The transcripts of the 35 genes measured by gene expression profiling (GeXP) multiplex reverse transcription–polymerase chain reaction (RT–PCR) were clustered to obtain a 4 × 4 grid of miniclusters according to their Euclidean distance as a measure of the similarity of the expression level of the genes relative to each other (panel lower right). Clustering was performed with a dataset representing all samples shown. The relative expression levels of the individual transcripts are colour coded. The relative position of each gene within the grid of miniclusters is identical in all GEDI maps shown. Plasmodia of wild type and mutants at 6 h after the onset of the far-red pulse are compared to the dark controls (DK). The sample ID number and whether the plasmodium has sporulated (+) on the next day or did not sporulate (–) is given at the left side of each map. Each map was computed from the expression pattern measured in a separate individual plasmdodial cell. The inset lower right indicates the assignment of the genes to each minicluster and the colour coding of the expression levels. Upregulated genes (printed in red) and downregulated genes (printed in green) were identified based on the Mann–Whitney U-Test.

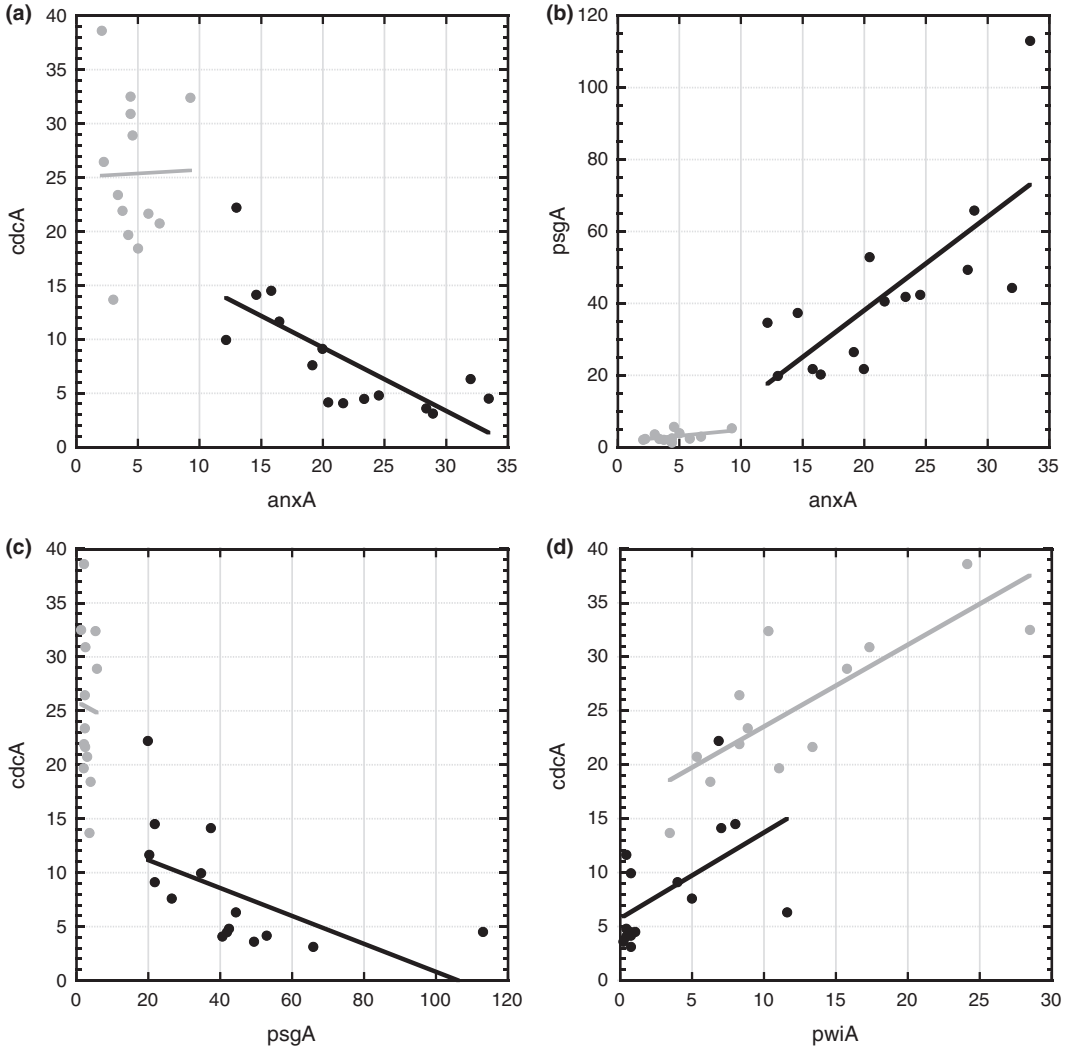

Fig. 4. Pairwise correlation of mRNAs measured in individual plasmodial cells of the wild type strain WT31. Each data point indicates the relative transcript abundance within one individual plasmodial cell without (black symbols) or 6 h after the onset of the far-red pulse (grey symbols). Straight lines were obtained by linear regression and are displayed solely to guide the eye.

psgA in wild type, for example, are inversely correlated and the correlation is only seen in plasmodia of the dark controls (Fig. 4), while *cdcA* and *pwiA* are positively correlated in the dark and in far-red irradiated plasmodia. As the overall correlation value of *cdcA*/*psgA* pair was below threshold, it is not seen in Figure 5.

In different mutants correlation patterns clearly differ from each other. In PHO72 plasmodia, for example, the number of correlations between genes has drastically increased. This is evident for the sporulated PHO72 plasmodia and even more pronounced in the non-sporulated plasmodia. A similar high degree of correlation is seen in PHO1 while the correlation patterns of PHO1 and PHO3 differ drastically, although the two strains appear to behave somewhat similarly according to the GEDI maps. In the sporulated plasmodia of PHO48 there is correlation among the up- and the downregulated genes, similar to wild type, but in the non-sporulated PHO48 plasmodia, most correlations are lost. Most interestingly, new correlations are found and some genes (in PHO57 and PHO64) are even inversely regulated by light as compared to the wild type. Hence, the non-sporulating mutants differ drastically from the wild type and from each other with respect to the expression correlation patterns of genes that are differentially regulated before and during commitment of the wild type to sporulation.

Discussion

We have isolated *Physarum polycephalum* mutants that do not sporulate in response to far-red light and performed quantitative analyses of the expression levels of a set of 35 genes with the help of GeXP multi-

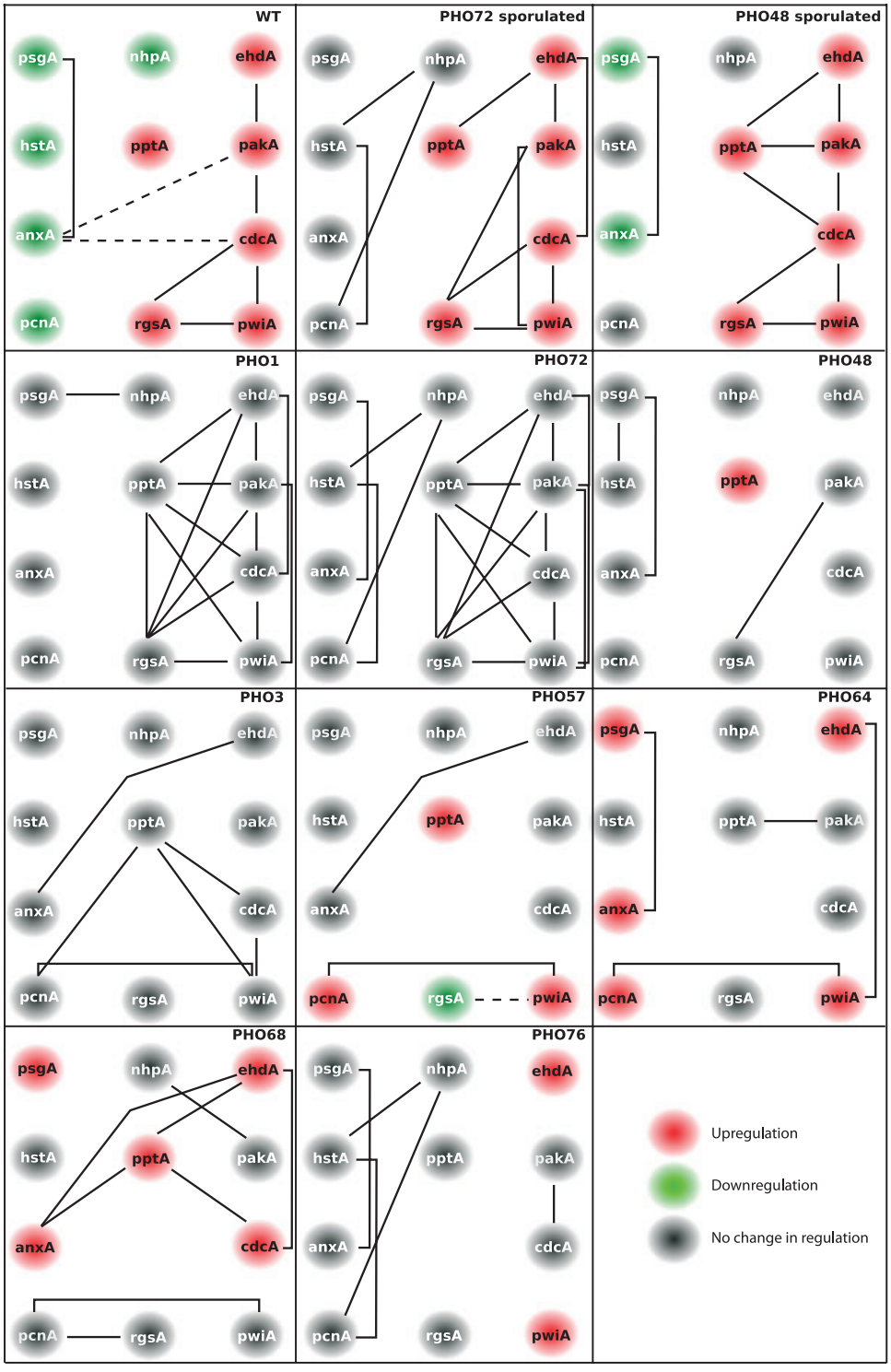

Fig. 5. Patterns of the correlated expression of differentially regulated genes in wild type and mutants. To search for pairwise correlation, the Pearson correlation between all 35 genes was calculated. Eleven genes that according to the Mann–Whitney U-test are differentially regulated in the wild type were selected from the miniclusters of the Gene Expression Dynamics Inspector (GEDI) maps for the graphical display of their degree of correlated expression. Lines connecting the gene symbols indicate a pairwise correlation coefficient of $r = 0.8$. Straight lines indicate positive and dashed lines negative correlation of the expression levels, respectively. Transcripts that were up- or downregulated with a confidence interval of ≥ 95 % (Mann–Whitney *U*-test) in the far-red irradiated plasmodia as compared to dark controls are marked in red or green, respectively.

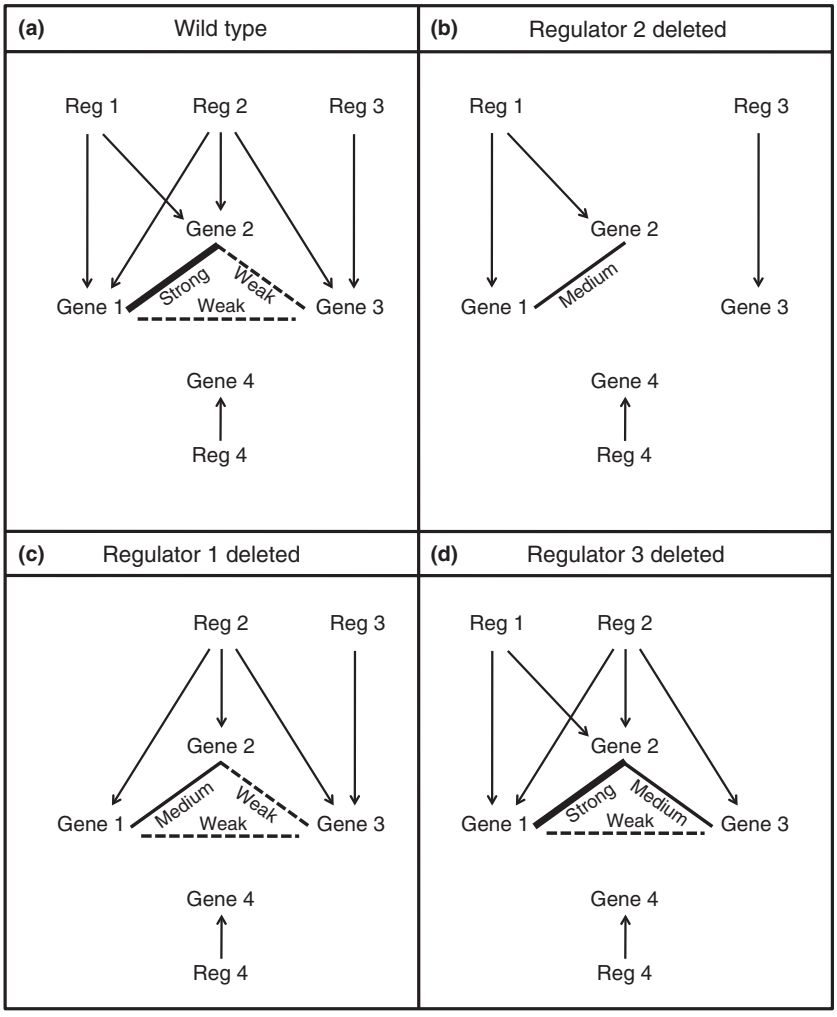

Fig. 6. Scheme proposing mechanisms to explain changes in the pairwise correlation of transcript abundance in response to the deletion of upstream regulators of the corresponding genes. According to the model, overlapping control of two regulators reveals strong correlation in expression. Control by one and the same regulator only causes medium correlation due to other influences. If two genes are controlled by the same regulator and one of them is in addition controlled by an independent regulator, the observed correlation in expression level is weak. The model gives a possible explanation of the observed phenomenon that the number of gene pairs with correlated expression level drastically increased in some of the sporulation-deficient mutants.

plex RT–PCR. The gene expression patterns were evaluated with GEDI (Eichler *et al.* 2003; Guo *et al.* 2006), a software package that clusters genes according to the similarity of expression patterns and visualizes the results with the help of self organizing map algorithms. GEDI maps of individual plasmodial cells indicated that the plasmodia of different non-sporulating mutants responded differently to the light stimulus as well as differently as compared to the wild type (Fig. 3). The GEDI maps also indicated that the gene expression pattern of unstimulated plasmodia (the dark controls) is altered in most of the mutants as compared to the wild type. Even without GEDI mapping it was obvious that the expression levels of some of the genes that are up- or downregulated in the wild type in response to light stimulation were relatively strictly pairwise correlated (Fig. 4). For some gene pairs correlation was not seen in far-red irradiated plasmodia, while it clearly occurred in the dark controls. Correlation was positive or negative, depending on the pair of genes considered. Despite being strongly correlated, the expression levels of some of these genes varied considerably (fivefold or more) between individual plasmodial cells of a given strain when compared to other, not regulated genes in the samples. The individual differences in gene expression patterns of individual plasmodia from the same strain are not due to inhomogeneities within a multinucleate plasmodium, as different samples taken from different parts of the same plasmodium show indistinguishable gene expression patterns (Rätzel and Marwan, unpubl. data, 2012). For a systematic evaluation of the pairwise correlation of transcript levels, we have chosen an arbitrary subset of 11 out of those genes that are strongly differentially regulated in the wild type and calculated the Pearson correlation for each gene as compared to each other out of the set. This analysis revealed that the different mutants displayed different patterns of pairwise correlation (Fig. 5). In some of the mutants, the number of pairwise correlations

increased. In other mutants the number of correlations decreased and new patterns of pairwise correlation formed. These results suggest that patterns of correlation in the expression levels of pairs of genes can be used to functionally characterize non-sporulating mutants. In summary, there are three molecular criteria to phenotypically discriminate non-sporulating mutants: (i) the gene expression pattern in unstimulated cells; (ii) the differential regulation of genes in response to stimulation with far-red light; and (iii) the pattern of correlated expression of pairs of genes. Certainly, whether or not these phenotypic traits are specific to the mutation that blocks light-induced sporulation has to be determined for each mutant individually.

How can mutations change the correlated expression of pairs of genes? A possible explanation is given in Figure 6. Let us assume that in the wild type, the transcript level of four genes is under the control of four regulators that are differently connected to the four genes (Fig. 6a). Each of the regulators may receive input from cellular processes while there is no direct or strict coupling between the four regulators. In the example shown, expression of Gene 4 is not correlated with the other three genes as it is controlled by its own regulator (Reg 4), which is neither linked to the other three genes nor to the other three regulators. The expression levels of Gene 1, Gene 2, and Gene 3 are more or less strongly correlated due to the partly overlapping regulatory control by Regulator 1, Regulator 2, and Regulator 3. If the highly connected Regulator 2 is deleted (Fig. 6b), the only correlation that is left is between Gene 1 and Gene 2 as mediated by Regulator 1. The correlation strength between the two genes may be somewhat weaker as in the wild type because the co-regulatory influence of Regulator 2 on the pair of genes is missing. When on the other hand, Regulator 1 (Fig. 6c) or Regulator 3 (Fig. 6d) are deleted, the strengths of pairwise correlations change due to the altered combinatorial influence of the respective regulators that have been disabled by the mutation. At a given threshold for the numerical value of the correlation of expression to be considered as significant, as it was set to prepare Figure 5, the number of correlating connections between the three genes changes accordingly. Based on this rationale it might be possible to reverse engineer (i.e., infer) the layers of regulatory control uncovered by the mutants from altered patterns in the correlated expression of pairs of genes as measured in individual plasmodial cells. In addition, GEDI analysis may assist reverse engineering approaches. To conclude, the experimental data suggest that the increase in the number of gene pairs with correlated expression level is due to the deletion of regulators or of their upstream components.

Acknowledgments

This work was financially supported by a BMBF FORSYS grant and by the Excellence Initiative of Saxony Anhalt. We thank Dr Joseph Zhou for help with the GEDI analysis and for critical reading of the manuscript. We also thank Mrs Bärbel Lorenz and Mrs Regina Pflug for excellent technical assistance.

References

Anderson, R. W., Dee, J. & Foxon, J. L. 1997. G1-phase arrest is not a prerequisite for encystment in *Physarum*. *Exp. Cell Res.* **236**, 351–354.

Bailey, J. 1995. Plasmodium development in the myxomycete *Physarum polycephalum*: genetic control and cellular events. *Microbiology* **141**, 2355–2365.

Bailey, J., Anderson, R. W. & Dee, J. 1987. Growth and development in relation to the cell cycle in *Physarum polycephalum*. *Protoplasma* **141**, 101–111.

Bailey, J., Solnica-Krezel, L., Anderson, R. W. & Dee, J. 1992. A developmental mutation (*npfL1*) resulting in cell death in *Physarum polycephalum*. *J. Gen. Microbiol.* **138**, 2575–2588.

Baldauf, S. L. & Doolittle, W. F. 1997. Origin and evolution of the slime molds (*Mycetozoa*) *Proc. Natl Acad. Sci. USA* **94**, 12007–12012.

Baldauf, S. L., Roger, A. J., Wenk-Siefert, I. & Doolittle, W. F. 2000. A kingdom-level phylogeny of eukaryotes based on combined protein data. *Science* **290**, 972–976.

Barrantes, I., Glöckner, G., Meyer, S. & Marwan, W. 2010. Transcriptomic changes arising during light-induced sporulation in *Physarum polycephalum*. *BMC Genomics* **11** 115.

Burland, T. G., Solnica-Krezel, L., Bailey, J., Cunningham, D. B. & Dove, W. F. 1993. Patterns of inheritance, development and the mitotic cycle in the protist *Physarum polycephalum* *Adv. Microb. Physiol.* **35**, 1–69.

Daniel, J. W. & Baldwin, H. H. 1964. Methods for culture of plasmodial myxomycetes. *Methods Cell Physiol.* **1**, 9–41.

Daniel, J. W. & Rusch, H. P. 1962. Method for inducing sporulation of pure cultures of the myxomycete *Physarum polycephalum*. *J. Bacteriol.* **83**, 234–240.

Dee, J. 1966. Multiple alleles and other factors affecting plasmodium formation in the true slime mold *Physarum polycephalum* Schw. *J. Eukaryot. Microbiol.* **13**, 610–616.

Dee, J. 1986. The culture of *Physarum* amoebae in axenic media. In: *The Molecular Biology of Physarum polycephalum* (eds W. F. Dove, J. Dee, S. Hatano, F. B. Haugli & K.-E. Wohlfarth-Bottermann), pp. 253–269. Plenum Press, New York.

Dee, J. 1987. Genes and development in *Physarum*. *Trends Genet.* **3**, 208–213.

Dee, J., Foxon, J. L., Hill, W., Roberts, E. M. & Walker, M. H. 1997. Contact with a solid substratum induces cycts in axenic cultures of *Physarum polycephalum* amoebae: mannitol-induced detergent-resistant cells are not true cysts. *Microbiology* **143**, 1059–1069.

Eichler, G. S., Huang, S. & Ingber, D. E. 2003. Gene Expression Dynamics Inspector (GEDI): for integrative analysis of expression profiles. *Bioinformatics* **19**, 2321–2322.

Guo, Y., Eichler, G. S., Feng, Y., Ingber, D. E. & Huang, S. 2006. Towards a holistic, yet gene-centered analysis of gene expression profiles: a case study of human lung cancers. *J. Biomed. Biotechnol.* **2006**, 1–12.

Hoffmann, X.-K., Tesmer, J., Souquet, M. & Marwan, W. 2012. Futile attempts to differentiate provide molecular evidence for individual differences within a population of cells during cellular reprogramming. *FEMS Microbiol. Lett.* **329**, 78–86.

Kroneder, R., Cashmore, A. R. & Marwan, W. 1999. Phytochrome-induced expression of *lig1*, a homologue of the fission yeast cell cycle checkpoint gene *hus1* is associated with the developmental switch in *Physarum polycephalum* plasmodia. *Curr. Genet.* **36**, 86–93.

Lamparter, T. & Marwan, W. 2001. Spectroscopic detection of a phytochrome-like photoreceptor in the Myxomycete *Physarum polycephalum* and the kinetic mechanism for the photocontrol of sporulation by P_{fr}. *Photochem. Photobiol.* **73**, 697–702.

Liu, W. & Saint, D. A. 2002. A new quantitative method of real time reverse transcription polymerase chain reaction assay based on simulation of polymerase chain reaction kinetics. *Anal. Biochem.* **302**, 52–59.

Mann, H. B. & Whitney, D. R. 1947. On a test of whether one of two random variables is stochastically larger than the other. *Ann. Math. Stat.* **18**, 50–60.

Martel, R., Tessier, A., Pallotta, D. & Lemieux, G. 1988. Selective gene expression during sporulation of *Physarum polycephalum*. *J. Bacteriol.* **170**, 4784–4790.

Mohberg, J. 1977. Nuclear DNA content and chromosome numbers throughout the life cycle of the Colonia strain of the myxomycete, *Physarum polycephalum*. *J. Cell Sci.* **24**, 95–108.

Putzer, H., Verfuerth, C., Claviez, M. & Schreckenbach, T. 1984. Photomorphogenesis in *Physarum*: induction of tubulins and sporulation-specific proteins and of their mRNAs. *Proc. Natl Acad. Sci. USA* **81**, 7117–7121.

Putzer, H., Werenskiold, K., Verfuerth, C. & Schreckenbach, T. 1983. Blue light inhibits slime mold differentiation at the mRNA level. *EMBO J.* **2**, 261–267.

Rai, A. J., Kamath, R. M., Gerald, W. & Fleisher, M. 2008. Analytical validation of the GeXP analyzer and design of a workflow for cancer-biomarker discovery using multiplexed gene-expression profiling. *Anal. Bioanal. Chem.* **393**, 1505–1511.

Rovine, M. J. 1997. A 14th way to look at a correlation coefficient: correlation as the proportion of matches. *Am. Stat.* **51**, 42–46.

Rusch, H. P., Sachsenmaier, W., Behrens, K. & Gruter, V. 1966. Synchronization of mitosis by the fusion of the plasmodia of *Physarum polycephalum*. *J. Cell Biol.* **31**, 204–209.

Sachsenmaier, W., Remy, U. & Plattner-Schobel, R. 1972. Initiation of synchronous mitosis in *Physarum polycephalum*. *Exp. Cell Res.* **73**, 41–48.

Schedl, T. & Dove, W. F. 1982. Mendelian analysis of the organization of actin sequences in *Physarum polycephalum*. *J. Mol. Biol.* **160**, 41–57.

Starostzik, C. 1995. Die Sporulation in *Physarum polycephalum*: Physiologische Charakterisierung einer verzweigten Signalkette (Dissertation). Ludwig-Maximilians-Universität, München.

Starostzik, C. & Marwan, W. 1994. Time-resolved detection of three intracellular signals controlling photomorphogenesis in *Physarum polycephalum*. *J. Bacteriol.* **176**, 5541–5543.

Starostzik, C. & Marwan, W. 1995a. A photoreceptor with characteristics of phytochrome triggers sporulation in the true slime mould *Physarum polycephalum*. *FEBS Lett.* **370**, 146–148.

Starostzik, C. & Marwan, W. 1995b. Functional mapping of the branched signal transduction pathway that controls sporulation in *Physarum polycephalum*. *Photochem. Photobiol.* **62** 930–933.

Starostzik, C. & Marwan, W. 1998. Kinetic analysis of a signal transduction pathway by time-resolved somatic complementation of mutants. *J. Exp. Biol.* **201**, 1991–1999.

Sujatha, A., Balaji, S., Devi, R. & Marwan, W. 2005. Isolation of *Physarum polycephalum* plasmodial mutants altered in sporulation by chemical mutagenesis of flagellates. *Eur. J. Protistol.* **41**, 19–27.

Werenskiold, A. K., Schreckenbach, T. & Valet, G. 1988. Specific nuclear elimination in polyploid plasmodia of the slime mold *Physarum polycephalum*. *Cytometry* **9**, 261–265.

Wheals, A. G. 1970. A homothallic strain of the myxomycete *Physarum polycephalum*. *Genetics* **66**, 623–633.